

(11) **EP 4 481 089 A2**

(12)

EUROPEAN PATENT APPLICATION

(43) Date of publication: 25.12.2024 Bulletin 2024/52

(21) Application number: 24174126.3

(22) Date of filing: 03.05.2024

(51) International Patent Classification (IPC):

C25D 11/08^(2006.01)
C25D 11/24^(2006.01)
A61L 27/06^(2006.01)
C25D 11/26^(2006.01)
C25D 11/26

(52) Cooperative Patent Classification (CPC): C25D 11/08; A61L 27/06; C25D 11/24; C25D 11/26

(84) Designated Contracting States:

AL AT BE BG CH CY CZ DE DK EE ES FI FR GB GR HR HU IE IS IT LI LT LU LV MC ME MK MT NL NO PL PT RO RS SE SI SK SM TR

Designated Extension States:

BA

Designated Validation States:

GE KH MA MD TN

(30) Priority: 03.05.2023 US 202363499717 P

(71) Applicants:

• Tesler, Alexander 91056 Erlangen (DE)

Goldmann, Wolfgang H.
 91054 Erlangen (DE)

(72) Inventors:

 TESLER, Alexander 91056 Erlangen (DE) GOLDMANN, Wolfgang 91054 Erlangen (DE)

 PRADO, Lucia H. 04107 Leipzig (DE)

MAZARE, Anca
 90408 Nürnberg (DE)

• THIEVESSEN, Ingo 91056 Erlangen (DE)

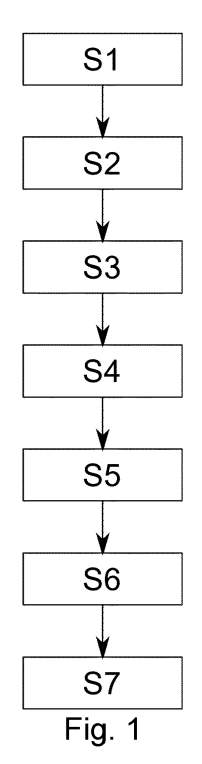
BÖHRINGER, David
 91078 Herzogenaurach (DE)

SANTIAGO, Callum E.
 69118 Ziegelhausen (DE)

(74) Representative: FDST Patentanwälte Nordostpark 16 90411 Nürnberg (DE)

(54) METHOD FOR PREPARATION OF A SURFACE, METHOD FOR CHARACTERIZATION OF A SURFACE, COMPONENT, AND USE OF SUCH COMPONENT

(57)A method is described for the preparation of a surface (2) such that it thermodynamically stable traps air when immersed in aqueous media, comprising the steps of: Providing a material, wherein the said material comprises the said surface (2); Connecting the material as a working electrode (4); Providing an electrolyte (6); Addition of H₂O₂ to the electrolyte (6); Providing a counter electrode (8); Applying a pre-defined voltage (V), wherein, upon application of the voltage (V), anodization of the working electrode (4) is carried out over a pre-defined time interval; Functionalizing the material by bringing it into contact with a fluorinated agent (10) and heating it to a pre-defined temperature. In addition, a method for characterizing a surface (2), a component (14), and uses for a component (14) are described.



EP 4 481 089 A2

Description

10

20

30

35

45

50

55

[0001] The invention concerns a method for preparation of a surface, a method of characterization of a surface, a component with such a surface, and the use of such a component.

[0002] Wetting describes the ability of liquids to maintain contact with a solid surface. However, in engineering and medical applications, the contact of a solid surface with water can lead to undesirable phenomena such as corrosion, chemofouling and biofouling, which potentially have negative economic, health, and environmental effects. Therefore, controlling wetting on solid surfaces is key to mitigating its detrimental effects. Although wetting is a macroscopic process, it is sensitive to surface properties at the molecular level. Thus, wetting is also strongly influenced by surface topography. High surface roughness in combination with low-surface-energy materials lead to the formation of non-wettable, so-called super-hydrophobic surfaces (SHS). A special type of SHS, which combines a microscale/nanoscale (hierarchical) rough surface topography with low-surface-energy chemistry, can trap air between their protrusions when immersed in water, a situation termed a plastron, and such surfaces are also called aerophilic surfaces (APhS).

[0003] SHS are still rarely used in engineering applications mainly due to two drawbacks. First, highly textured rough surfaces are mechanically weaker than their smooth analogues and thus easily abraded. This drawback of SHS has recently been addressed, e.g., as described in Lu, Y. et al. "Robust self-cleaning surfaces that function when exposed to either air or oil" Science 347, 1132-1135 (2015). Second, a much less resolved drawback is that the non-wetting properties degrade over time due to the metastable performance of the plastron, which arises from the coexistence of different energy states. Such a metastable performance is even more critical when APhS are submerged in water, since the air trapped between the protrusions disappears over time. As a result, the long-term stability of such surfaces underwater is considered inadequate for many engineering applications, especially for biofouling prevention. Thus, the long-term stability of plastron remains the 'Achilles heel' in the implementation of technology involving SHS or APhS. Furthermore, it is even more challenging to produce mechanically robust SHS/APhS with stable plastron by a facile, inexpensive, and scalable process. According to Li et al. "Challenges and strategies for commercialization and widespread practical applications of superhydrophobic surfaces" Science Advances Vol. 9, No. 42 (2023), the comprehensive performances, preparation and characterization methods, and application scenarios of SHS are the major constraints in their wider commercialization.

[0004] To facilitate an understanding of the invention, it is helpful to explain various models of surface wettability. This area of research is not always used precisely, and in many cases does not provide sufficient surface characterization. The Young's model covers the wettability of atomically smooth solid surfaces of homogeneous chemistry, depending on the contact angle of water droplets to the surface in hydrophilicity (contact angle <90°) or hydrophobicity (contact angle >90°). According to the Young's equation, the maximal contact angle of water droplet rests on smooth hydrophobic surface can't exceed 120°. The Wenzel model showed that in the case of a hydrophobic surface, hydrophobicity increases due to the roughness of the surface; it describes the condition when the pores (or rough protrusions) of the surface are filled with liquid. The Wenzel wetting is represented by contact angles higher than 150°, but with low mobility of water (aqueous media) droplets on the Wenzel surface. The latter is represented by contact angle hysteresis or tilt/sliding angle that is a dynamic parameter of wetting. On the other hand, the Cassie-Baxter model describes the case when due to the specific surface roughness and hydrophobic (low surface tension/energy) coating, the interaction between the liquid and the surface is reduced due to air trapped between rough protrusions. In the Cassie-Baxter wetting regime, a water droplet experiences heterogeneous wetting, while it partially touches the top of solid rough protrusions, while the rest of the droplet is in contact with air. The shape of the droplet remains circular, while the low number of pinning points with the solid substrate leads to their rapid rolling off from the surface leaving behind a clean wetting-free surface. The low amount of pinning points leads to a very high water contact angle and very low contact angle hysteresis, i.e., very low friction. The term super-hydrophobicity is used to describe a condition in which a roll-off angle of <10° (some literature say a value <5°) is added to the water contact angle of >150°. The air layer that forms on the solid surface, while the surface is submerged underwater, is termed 'plastron'. It is the current consensus that plastron on artificially made superhydrophobic surfaces can only be metastable. Yet, in other publications the term 'plastron' is not always defined or used according to this understanding; it usually includes states, which are characterized macroscopically by very low wettability, even without further differentiation, i.e., without further distinction as to whether it is a Wenzel or a stable or metastable Cassie-Baxter state. Also, it is noted that there are also substances that exhibit strong adhesion for water despite a contact angle of >150°, i.e., the rose petal effect.

[0005] Reference is made to US 2006 / 0 029 808 A1, US 2007 / 0 005 024 A1, US 2014 10 238 263 A1, and CN 108 486 633 A. Reference is also made to Gao et al. "Facile fabrication of superhydrophobic surfaces with low roughness on Ti-6Al-4V substrates via anodization", Applied Surface Science 314 (2014) 754-759.

[0006] First, the object of the invention is to provide a surface with improved hydrophobicity/aerophilicity. Second, another object is to provide a surface, which is prepared to sustain stable plastron as long as possible, e.g., for several months. Third, another object is to provide a long-term stable aerophilic blood-repellent metallic surface. Fourth, another object is to provide a titanium alloy surface on which a plastron can be formed, and which is stable over several days.

Fifth, another object is to permanently stabilize an air layer on a surface underwater. In other words: super-hydrophobicity is necessary but not sufficient; stable long-term hydrophobicity is desired. Further, another object is to provide a titanium alloy with an aerophilic surface, which is reusable, stable against environmental influences, and at the same time cheap. Correspondingly, a suitable method for preparing such a surface, a component comprising such a surface, as well as applications, i.e., uses for such a surface shall be described.

[0007] One or several of the objects mentioned herein are solved by a method with the features according to claim 1, a method with the features according to claim 11, a component with the features according to claim 12 and a use with the features according to claim 15. Advantageous embodiments are the subject of the dependent claims. Any description relating to the methods applies mutatis mutandis to the component and use and vice versa.

[0008] One inventive method is a methodology for preparation of a surface, such that it becomes an aerophilic surface, which is advantageously stable for at least two days. The method comprises the following seven steps:

First step: Providing a material. Preferably, the material is a metal-containing material, suitable materials are a titanium alloy, more preferably alpha-beta titanium aluminum vanadium alloy, more preferably Ti-6Al-4V. However, other metal-containing materials, in particular metals itself, such as zinc, magnesium, copper, iron, nickel, or aluminum and their alloys, are also suitable as material. Also suitable materials are metal-oxides and ceramics. In general, a solid material with a high surface roughness is desired as material. In the following, it will be assumed without loss of generality that the material is a metal-containing material, specifically a titanium alloy. The said metal-containing material comprises the said surface, which in the following is prepared to exhibit improved aerophilicity, which in turn also means improved hydrophobicity. The said surface is a solid surface.

Second step: Connecting the material and, hence, also its surface, as a working electrode (anode).

Third step: Providing an electrolyte, preferably a NaOH solution, e.g., 1.5 M NaOH.

Fourth step: Addition of H_2O_2 to the electrolyte, preferably 1 vol%.

10

15

20

25

30

35

40

50

Fifth step: Providing a counter electrode (cathode), preferably made of steel, preferably of either 304 or 316 grade. With the first to the fifth step, thus, an electrochemical anodization setup is provided, with the material as an anode (working electrode), the counter electrode as the cathode and an aqueous solution of NaOH (as electrolyte) and H_2O_2 . The electrodes and the electrolyte form an electrochemical cell. Before anodization (sixth step, see below) the surface is preferably cleaned, e.g., ultrasonically in acetone and ethanol for 10 min to remove any contamination but the same process will be equally applied also on the naturally contaminated substrates or the substrates precleaned in regular soap solution. In general, however, cleaning is not necessary, in particular due to the combination of NaOH/ H_2O_2 acting as a strong oxidizer and the generally harsh atmosphere during anodization. If any, cleaning with simple soap will usually suffice. The electrodes are preferably placed 10 mm to 100 mm away from each other depending on the sample size.

Sixth step: Applying a pre-defined voltage, wherein, upon application of the voltage, anodization of the working electrode is carried out over a pre-defined time interval. This yields an as-anodized surface. The said time interval is preferably at least 5 min, preferably at least 30 min, preferably at most 60 min, preferably in the range from 10 min to 60 min. The said voltage is preferably larger than 10 V and smaller than 20 V, and most preferably 15 V. In a suitable embodiment, the said voltage is 15 V + 7.5 V.

[0009] The electrochemical cell may suitably be kept in a reservoir of water at room temperature or in a reservoir with ice. The anodization can be repeated up to three times with the same electrolyte.

[0010] To achieve a high roughness of the surface, it is preferred that the method is conducted such that two reactions occur simultaneously, namely an electrochemical oxidation of the surface to form a microscale rough oxide layer (first reaction), and a chemical dissolution (i.e., etching) of the formed oxide in the same electrochemical environment to increase porosity and create nanoscale roughness (second reaction).

[0011] Preferably, the material is washed and/or dried after removal from the electrolyte and after the sixth step. For example, the surface is removed from the electrolyte, and as-anodized rinsed with deionized water (or ethanol) and/or dried under a stream of N_2 .

[0012] Seventh step: Functionalizing, in particular low surface energy functionalizing, the material, in particular the surface, by bringing it into contact with a fluorinated agent (surfactant) and heating it to a pre-defined temperature. By this method, the surface of the material is fluorinated and, thus, functionalized, i.e., its aerophilicity is gained. The said functionalizing yields a low-surface-energy material, in particular titanium aerophilic surface (APhS). The said temperature is preferably in the range from 20 C to 70 C, more preferably 50 °C to 70 °C. Heating is suitably achieved by placing the

material in a furnace, e.g., muffle furnace. The fluorinated agent preferably comprises or is a fluorinated phosphonic acid ester. A fluorinated phosphonic acid ester is cheap and stable. Another advantage of a fluorinated phosphonic acid ester is that it forms (as part of the method described here) a self-assembled monolayer that facilitates formation of a thermodynamically stable plastron on the surface. A suitable fluorinated agent is FS-100 (perfluoroalkyl phosphate acid ester), preferably dissolved in 1 liter of 95:5 vol% ethanol/H₂O by ultra-sonication and kept under ambient conditions. As-anodized samples are immersed in this FS solution. The said time interval preferably is at least 10 min, preferably at least 30 min, preferably at most 60 min, preferably in the range from 10 min to 60 min.

[0013] After low surface energy functionalizing, the material is preferably rinsed, e.g., with ethanol, and/or dried, e.g., under a stream of N₂ or via natural drying or similar.

[0014] In a suitable embodiment, the fluorinated surface is exposed multiple times to fresh blood (outside the human/animal body and without intervention with the human/animal body). In particular, this is done to assess the performance of the surface.

[0015] The inventive method yields a substrate, preferably a metallic substrate, with a surface which is aerophilic and/or in the thermodynamically stable Cassie-Baxter state, and which is, hence, stable for at least two days, more preferably at least 2, 10, or 12 months or longer. In summary, a method (methodology) is presented to form surfaces with a long-term stably trapped air layer on the surface during the immersion in aqueous media. The invention aims to obtain and achieves solid substrates less susceptible to various types of decomposition and/or contamination that can occur on the surface in a humid and/or liquid environment and/or in a living body. In a first part of the said method, the surface to be treated, e.g., a titanium alloy and, is immersed in an electrolyte, and electrochemical anodization is applied. This roughens the surface forming a hierarchical structure, which has irregularities on a length scale of micrometers, within which smaller unevenness is formed on a nanometer scale. This provides the solid surface with a high surface area, which is above minimal roughness for thermodynamic stability of plastron. In a second part of the said method, a special agent is applied to the thus structured surface, which advantageously forms a uniform monolayer increasing the solid surface hydrophobicity.

[0016] In addition, a method (methodology) is presented to characterize a surface in terms of surface roughness, liquid-solid area fraction, and most stable contact angle or the most stable contact angle equivalent emphasizing particular conditions that enable long-term stable air trapping on solid metallic surfaces. Noting that in general Young's contact angle is not a measurable value and the most stable contact angle as its replacement is also not a common measurement, since there is no common way to measure it, it is replaced by the most stable, advancing and receding contact angles measured on a flat surface of the same hydrophobic origin. The most stable, advancing and receding contact angles represent the minimal and maximal apparent contact angle limits available on the corresponding solid surface, including inside Young's and the most stable contact angles. Correspondingly, in a suitable embodiment the surface's roughness, liquid-solid area fraction (=portion of the surface that is in actual contact with the solid surface), and/or the most stable, advancing and receding contact angles is/are determined, in particular measured, and a long-term stability of air trapping on the surface is characterized based on the roughness, liquid-solid area fraction, and/or most stable, advancing and receding contact angles. In this way, the thermodynamic stability of the functionalized surface (e.g., APhS) is assessed. Thermodynamic (long-lasting) stability of plastrons is preferably characterized by wetting-resistance performance preserved under the application of external stimuli such as change in temperature, hydrostatic and hydrodynamic pressure, or vibration of construction. This is in contrast to alternative approaches, which exclusively use the contact angle (CA) and/or contact angle hysteresis (CAH), which cannot correctly describe a wetting regime. Note - based on previous literature, plastrons have been termed "ultra-stable" for the period of immersion in deionized water of 30 days (Thamaraiselvan et al., Superhydrophobic candle soot as a low fouling stable coating on water treatment membrane feed spacers. ACS Appl. Bio Mater. 4, 4191-4200 (2021)), while periods longer than 50 days have been termed as "infinitely stable plastrons" (Xu et al., Infinite lifetime of underwater superhydrophobic states. Phys. Rev. Lett. 113, 136103 (2014)).

30

35

45

50

[0017] Experiments with the surface as prepared by the inventive method have shown that the said surface is principally capable of retaining an air film underwater for more than 10 to more 12 months or even longer of continuous immersion. Also, repeated immersion in blood leaves no residue on the surface. Experimental confirmation has also been published by Tesler at al. "Long-term stability of aerophilic metallic surfaces underwater" Nature Materials, Volume 22, December 2023, 1548-1555.

[0018] The invention is beneficial in several areas of application, in particular where titanium alloys are already used and/or where an aerophilic (thermodynamically stable Cassie-Baxter superhydrophobic) surface is advantageous, particularly in medicine (implants), but also in aerospace (frost-free), or the marine sector (corrosion-free and biofouling-free surfaces).

[0019] As described, a suitable embodiment of the preparation method comprises preparation of a surface of a material as a particularly aerophilic surface. Advantageously, the said surface is prepared as a blood-repellent surface. In a suitable embodiment, the aerophilic surface is formed on an easily available titanium alloy, preferably Ti-6AI-4V composed of 90% titanium, 6% aluminum, and 4% vanadium. The said surface is, therefore, referred to as Ti-APhS and results in an unprecedented plastron stability exceeding 365 days of continuous submersion underwater (Tesler et al., submitted,

not yet published). The preparation of the surface is possible by an industry-standard electrochemical anodization technique followed by modification with a commercially available fluorinated surfactant. The prepared Ti-APhS is extremely blood repellent and drastically reduces or prevents the adhesion of bacteria and marine organisms such as mussels and barnacles. The inventors have found by thermodynamic calculations, that in contrast to previous understanding, thermodynamically stable plastrons underwater are feasible and can exist. The surface roughness and interfacial energy resulting from the inventive method give rise to a thermodynamically stable aerophilic regime, as has been verified by the inventors using existing theories, e.g., theories described by Marmur, A. "Underwater super-hydrophobicity: theoretical feasibility" Langmuir 22, 1400-1402 (2006) and Lafuma, A. & Quéré, D. "Superhydrophobic states" Nat. Mater. 2, 457-460 (2003). The present invention provides experimental evidence and confirmation of the theory, demonstrating that long-term entrapment of air on engineered SHS is feasible for a wide range of applications.

10

20

30

35

40

50

55

[0020] Identifying the specific factors that govern the stability of the plastron and the resulting performance of SHS underwater is challenging. This is due to the large variety of designs present in both natural and artificially made SHS as well as the lack of standardized measurement protocols and equipment, a deficit, which is overcome by the present invention. Yet, it is crucial to anticipate the performance of SHS underwater through simple and widely accessible methods. In the inventive method for characterizing a surface as presented here this is achieved by the characterization of specific sets of features that are responsible for performance differences of SHS underwater for closely related treatment systems. Preferably, a facile reflectance microscopy technique is used. In a particularly suitable embodiment, the surface is submerged in a liquid, upon which a plastron forms on the surface, wherein shape of the plastron and/or coverage of the surface with the plastron are estimated using optical reflection microscopy on the submerged surface. Preferably, the plastron shape and coverage are estimated using digital still imaging and bright-field optical reflection microscopy on the submerged surface. To demonstrate the general applicability of the method, two sets of SHS with plastron are prepared: (i) the same hydrophobic molecule coating but different anodized Ti surface morphologies, named Ti-SHS1-FS and Ti-SHS2-FS, and (ii) the same anodized Ti surface morphology but different hydrophobic coatings, named Ti-SHS1-FS and Ti-SHS1-Sil. In a suitable embodiment, the stability of the plastron and surface coverage are then assessed over time by immersing SHS in water. The optical reflectance microscopy measurement provides plastron shape and surface coverage, i.e., the solid-liquid area fraction and a change over a millimeter scale range. With such a setup, plastron instability is easily obtained within minutes.

[0021] While some steps or agents may appear to be standard elsewhere, the methods presented here, and the agents used therein have not been presented previously. One particular simplification that a particular embodiment of the preparation method provides, is the use of steel as counter electrode instead of, e.g., platinum. While steel is easily accessible and cheap, it has up to now not been used in the context as described here. This allows simple and cheap scaling of the method in terms of anodized area and electrode geometry (round, cylindrical, etc.), instead of restricting it to a laboratory scale. For example, large steel electrodes with dimensions of 100 mm to 200 mm or larger to match the working electrodes size are simple and cost effective. Also, a particular embodiment of the method as presented here uses heretofore unused hydrophobic molecules (fluorinated phosphonic acid ester) to prepare the surface such that it is in fact thermodynamically stable.

[0022] The invention has benefits in several applications, in which a surface, in particular of a metal, such as titanium alloy is used. Preferred applications in which a surface as prepared by the inventive method is used are medical applications, in particular implants and prostheses, aerospace applications, in particular stressed components in aerospace applications, marine applications, applications in the chemical industry, application in a gas turbine. When used for medical applications, the high biocompatibility of a medical implant having a surface as described here is an advantage. This includes the fact that the preferably used metal hardly interacts chemically with the body; it has further a density similar to that of human bone and unlike many other materials allows direct bonding to bone tissue without being adhesive. An additional advantage of titanium (and similar materials) is that it is not ferromagnetic and, therefore, does not interfere with MRI examinations. In addition to its application for implants, titanium is also used for some surgical tools. In general, the aerophilic surfaces will reduce the risk of infection; bacteria cannot adhere to the implant that has been treated according to the invention. This in turn will reduce the risk of infection at the surgical site of the implant.

[0023] An inventive component comprises a surface which has been prepared using the method as described above. Such a surface is advantageously in a thermodynamically stable Cassie-Baxter state. The surface is, by virtue of the specific preparation, configured to be covered by a thermodynamically stable air layer when immersed in an aqueous medium. Correspondingly, an inventive component comprises a surface configured to be covered by a thermodynamically stable air layer when immersed in an aqueous medium. In a suitable embodiment, the component is a medical implant. [0024] As such, the surface when used is in fact covered by a thermodynamically stable air layer (stable plastron) when immersed in an aqueous medium. In particular, the expression "thermodynamically stable" is understood as "stable for at least several months, e.g., for at least 2, 10, or 12 months", as already indicated above. In general, "thermodynamically stable" is understood here as the surface not easily getting wet due to small perturbations, e.g., in temperature, pressure or vibration.

[0025] While titanium alloy has been mentioned above as a preferred example for the material, other materials are

suited as well. In the following, aluminum is described as another preferred choice for the material and in order to prove the general viability of the invention. The description also applies to aluminum oxides. Using aluminum as the material, micro-nanostructures are preferably fabricated first by (i) chemical etching in an aqueous 3 M hydrochloric acid (HCI) solution of sequentially etched (two-step etching) for 2 min at 40 °C, followed by 1 min at 80 °C (Fig. 11a1)(E-AI) followed by (ii) electrochemical anodization (EA-AI) in an aqueous oxalic acid electrolyte at 1 °C for 1 min under an applied voltage of 60 V (Fig. 11a2). The surface of the material is coated with a fluorinated agent, preferably FS. The resulting functionalized material is termed E-AI/FS and EA-AI/FS for the etched and etched/anodized specimens, respectively. The static contact angles are measured and found to be 171.4° ± 7.6° and 169.8° ± 9.0° for E-AI/FS and EA-AI/FS, respectively (Fig. 11 c, inset images). Both types of AI-SHS exhibit a Cassie-Baxter wetting regime with comparable advancing and receding contact angles resulting in the landed drops rolling off instantly. The roughness parameter is preferably measured with atomic force microscopy yielding values of $r_{\text{E-Al/ES}}$ = 1.65 \pm 0.19 and $r_{\text{EA-Al/ES}}$ = 3.44 \pm 0.07 (Fig. 11d). The plastron shape and coverage are suitably estimated using digital still imaging and bright-field optical reflection microscopy on the submerged samples. Using a digital still camera, i.e., macroscopic measurements of plastron, both E-Al/FS and EA-AI/FS exhibit highly reflective surfaces underwater due to plastrons that cover the entire specimen area. In contrast, the bright-field optical reflection microscopy images, i.e., microscopic measurements of plastron, reveal a completely different plastron shape and solid-liquid area fraction. While the plastron on EA-AI/FS is continuous with randomly distributed round pinning points and a solid-liquid area fraction of ϕ_s = 0.16 \pm 0.08 (Fig. 11c2), the E-Al/FS demonstrated an irregular shape with a solid-liquid area fraction of only ϕ_s = 0.75 \pm 0.03 (Fig. 11c1). The latter is due to the deficiency of oxide/hydroxide groups resulting in the low FS coverage, which fails to form a thermodynamically stable plastron, i.e., with the liquid-air interface at the top of the asperities. Finally, the most stable contact angle (θ^{Si}_{MS}) was obtained previously for Ti-APhS and compared to the advancing (θ^{Al}_{Adv} = 121.9° \pm 3.4°) and receding (θ^{Al}_{Rec} = 74.9° \pm 5.7°) contact angles on the FS-coated polished Al samples. While the advancing contact angles on both surfaces are similar, the receding contact angle on the polished AI is much lower due to the higher surface roughness on AI. With the measured solidliquid area fraction and roughness parameter, the critical contact angle was calculated according as $\cos(\theta_c) = (\phi_s - 1)/(r$ - ϕ_s) and was found to be $\theta c = 93.5^{\circ}$ for EA-Al/FS. By comparing the MSCA (most stable contact angle) and critical contact angle, it is predicted that EA-AI/FS are in a stable Cassie-Baxter wetting regime (Fig. 11e). Using r> $(-1)/(\cos(\theta))$ + ϕ_s (1+ 1/(cos(θ)))= r_{min} , the stability of plastron underwater is estimated on EA-AI/FS, also predicting stable plastron (Fig. 11f). The mechanical characteristics of the E-AI/FS and EA-AI/FS specimens, previously examined using a nanoindentation technique, revealed values of hardness comparable to those of bare Al and elastic modulus in the gigapascal (GPa) range. Both E-Al/FS and EA-Al/FS were immersed in sea water for a period of several months. Based on the apparent contact angle and contact angle hysteresis parameters, both types of SHS should perform similarly to resist corrosion of AI in sea water. However, drastic difference was observed, while the E-AI/FS specimens demonstrated pronounced appearance of corrosion products already after 16 days of immersion in sea water due to rapid loss of plastron and the exposure of high surface area aluminum surface to the corrosive medium (Fig. 12a-b), while the EA-AI/FS specimens have not shown any sign of corrosion even after 234 days of immersion in sea water due to the fulfillment of both conditions, i.e., roughness above critical and hydrophobic coating by the FS - both lead to the formation of thermodynamically stable plastron on the EA-AI/FS specimens only (Fig. 11h) (Tesler et al., submitted, not yet pub-

10

15

20

30

35

40

[0026] Embodiments of the invention are now described with reference to a drawing with the following figures:

```
Fig. 1
                      a method,
      Fig. 2a
                      a setup used in the method of Fig. 1,
      Fig. 2b
                      another setup used in the method of Fig. 1,
      Fig. 3
                      a component with a surface,
      Figs. 4a-f
                      physiochemical characteristics of Ti-APhS
      Figs. 5a-e
                      HR-SEM and EDX spectrum of the anodized Ti surface after fluorination,
      Figs. 6a-h
                      various measurements and/or calculations,
      Figs. 7a-f
                      images of Ti-APhS with an artificially introduced bubble,
      Figs. 8a-j
                      various images and measurements,
50
      Figs. 9a-g
                      various bright-field reflectance microscopy images,
      Fig. 10a-d
                      bacterial repellence of Ti-APhS,
      Figs. 11a1-h
                      various measurements, calculations, and images relating to aluminum as metal-containing material,
      Figs. 12a,b
                      corrosion resistance of the E-AI/FS specimens immersed continuously in artificial seawater,
      Figs. 13
                      various measurements, calculations, and images,
      Figs. 14
                      various measurements, calculations, and images,
      Fig. 15
                      FS-100 (FS),
      Fig. 16
                      Laureth-4 Phosphate (Silaphos, Sil).
```

[0027] An exemplary embodiment of the inventive method is shown in Fig. 1. The method comprises a first step S1 of providing a material. The said material comprises a surface 2, which in the following is prepared to exhibit improved aerophilicity, which in turn also means improved hydrophobicity. In a second step S2, the material is connected as a working electrode 4 (anode). In a third step S3 an electrolyte 6 is provided, e.g., a 1.5 M NaOH solution. In a fourth step S4 H_2O_2 is added to the electrolyte 6. A fifth step S5 is providing a counter electrode 8 (cathode), e.g., made of steel. As such, an electrochemical anodization setup as shown in Fig. 2 is provided, with the material and its surface as the working electrode 4, the counter electrode 8 and an electrolyte 6. A sixth step S6 comprises applying a pre-defined voltage V, wherein, upon application of the voltage V, anodization of the working electrode 4 is carried out over a pre-defined time interval. This yields an as-anodized surface 2. The said time interval is, e.g., at least 5 min or at least 30 min. The said voltage V is, e.g., 15 V + 1 - 5 V.

[0028] To achieve a high roughness of the surface 2, the method is conducted such that two reactions occur simultaneously, namely an electrochemical oxidation of the metal surface 2 to form an oxide layer (first reaction), and a chemical dissolution of the formed oxide in the same electrochemical environment to increase porosity and create nanoscale roughness (second reaction).

[0029] In a seventh step, S7 the material, in particular the surface 2, is functionalized by bringing it into contact with a fluorinated agent 10 (reagent or surfactant) and heating it to a pre-defined temperature. An example of this is shown in Fig. 2b, in which a furnace 12 is used for the heating, while the surface 2 is at the same time immersed in the fluorinated agent. By this the surface 2 of the material is fluorinated and, thus, functionalized, i.e., its aerophilicity is improved. The said functionalizing yields a low-surface-energy material. The said temperature is, e.g., in the range from 20°C to 70 °C or 50 °C to 70 °C. In principle, it is possible to conduct the functionalization at room temperature, i.e., without additional heating, e.g., in a furnace, but higher temperatures speed up the process, thus, making it more feasible on an industrial scale.

[0030] Fig. 3 shows a component 14 comprising the material and its functionalized surface 2 submersed in water. With the surface 2 functionalized as described here, a stable plastron 16 is formed and that long-term and stable hydrophobicity is achieved when immersed in water (or similar liquids). This is further illustrated in Figs. 4-10. The presence of an intermediate air layer separates contaminating liquid such as blood from direct contact with the solid metallic surface preventing the adhesion of proteins and cells, Figs. 1-4. Figs. 5-6 demonstrate the blood-repellent characteristics of Ti surface obtained in the present invention. Figs. 7 demonstrate the ability of the Ti surface obtained in this invention to repel bacterial adhesion.

[0031] Physicochemical characteristics of Ti-APhS as obtained by the inventive method are shown in Figs. 4a-e. A high-resolution top-view scanning electron microscopy (increasing magnifications) is shown in Fig. 4a, atomic force microscopy images of Ti-APhS are shown in Fig. 4b. Figs. 4c, d show digital images of Ti-APhS prepared on sheets (Fig. 4c) and rod/coil (Fig. 4d) and demonstrate mirror-like reflectance underwater. The inset in Fig. 4d shows a Ti-APhS rod of 2 mm in diameter covered by plastron underwater. Fig. 4e shows EDS and Fig. 4f shows high-resolution X-ray photoelectron spectroscopy C 1s spectra of bare, as-anodized, and Ti-APhS.

[0032] Figs. 5a-d show HR-SEM and Fig. 5e shows EDX spectrum of the anodized Ti surface after fluorination, i.e., after the seventh step of the method.

[0033] Figs. 6a-h show various measurements and/or calculations as follows. Fig. 6a:

10

30

35

40

50

Top-view laser confocal, Fig. 6b scanning electron microscopy images, and Fig. 6c corresponding advancing and receding contact angle (CA) measured on p-TiHS. The image in Fig. 6c is a composite of advancing and receding CA measurements. The inset in Fig. 6a is a digital image of the polished FS-modified Ti alloy with mirror-like reflectance. Fig. 6d: Typical 3D reconstruction image of Ti-APhS roughness obtained by AFM. Fig. 6e: A typical bright-field reflectance microscopy image of Ti-APhS underwater; and Fig. 6f: A confocal cross-sectional image of plastron on Ti-SHS underwater. Fig. 6g: The apparent wetting contact angle (WCA) $\cos(\theta^*)$ as predicted by the Wenzel and Cassie-Baxter models as a function of the most stable WCA $\cos(\theta)$ based on the solid-liquid area fraction on Ti-APhS. The stable Cassie-Baxter wetting regime changes at the critical contact angle $\cos(\theta c)$ to a stable Wenzel or meta-stable Cassie-Baxter regime. The green area represents the possible wetting regimes of Ti-APhS measured on polished Ti (p-TiHS) and compared to the FS-modified Si/SiO2 wetting system (Si/SiO2/FS, yellow area). Fig. 6h: Minimum roughness (r_{min}), measured by AFM, optical profilometer, and laser confocal microscopy on Ti-APhS, required for a stable plastron underwater for ϕ_{s_max} = 0.011 (corresponding to the upper limit of liquid-solid area fraction) as a function of the most stable WCA (Θ)

[0034] Figs. 7a-f show digital images of Ti-APhS with an artificially introduced bubble covered by 1 cm de-ionized water. Fig. 7a shows an air bubble at day 0, and the following Figures after 78 (Fig. 7b), 91 (Fig. 7c), 130 (Fig. 7d), 208 (Fig. 7e), and 329 (Fig. 7f) days underwater. Water levels were kept constant during the duration of the experiment.

[0035] Figs. 8a-j show as follows: Contact angle (CA) of fresh blood on (Fig. 8a) as-anodized and (Fig. 8b) Ti-APhS. Fig. 8c: Advancing and receding CA measurements on Ti-APhS. Inset images: Droplet shape during increasing and decreasing blood droplet volume. Fig. 8d: Snapshot digital images of the blood droplet wiped off from Ti-APhS by paper tissue. Fig. 8e: Digital images of Ti-APhS before, during, and after 99 times of immersion in fresh blood. Fig. 8f: Blood

dripped on Ti-APhS shown in Fig. 8e. Figs. 8g-h: Ti-APhS after immersion in fresh blood for (Fig. 8g) 10 s and (Fig. 8h) 60 s. Figs. 8i-j: Still digital images of the sample immersed in fresh blood for 3,600 s (Fig. 8i), followed by a brief rinse in water (Fig. 8j).

[0036] Figs. 9a-g show bright-field reflectance microscopy images of (Figs. 9a-b) bare Ti alloy surface (Fig. 9a), and after exposure to blood for 1 s (Fig. 9b), Figs. 9c-d: Ti-SHS before (Fig. 9c) and after (Fig. 9d) exposure of 99 times to blood, and Figs. 9e-g: Ti-SHS before (Fig. 9e), after exposure of 1.8 h to blood (Fig. 9f), and after a brief rinse in water (Fig. 9g).

[0037] Figs. 10a-d show bacterial repellence of Ti-APhS. Fig. 10a: Time-lapse images of non-motile live GFP-expressed E. coli on bare, as-anodized, and Ti-APhS. Scale bar: 10 μ m. Fig. 10b: Surface coverage on the samples shown in Fig. 10a. Line width indicates mean +/- standard deviation measured from three independent biological replicates. Fig. 10c shows images and Fig. 10d surface coverage of non-motile bacteria on samples shown in Fig. 10a after 4 h of bacterial exposure and subsequent washing. The bracket denoted with ** in Fig. 10d indicates p<0.01 obtained by a two-sided student t-test. The scale bar in Figs. 10a, c is 10 μ m.

[0038] Figs. 11a1-h and 12a-b illustrate results using the inventive method with aluminum as the material. Micronanostructures are fabricated first by (i) chemical etching (E-AI,) followed by (ii) electrochemical anodization (EA-AI) as shown in Figs. 11a1-2. The surface of the material is coated with a fluorinated agent, here FS. The resulting functionalized material is termed E-Al/FS and EA-Al/FS for the etched and etched/anodized specimens, respectively, see Fig. 11b. The static contact angles are measured and found to be 171.4° \pm 7.6° and 169.8° \pm 9.0° for E-AI/FS and EA-AI/FS, respectively, as illustrated in Fig. 11c1-c2, inset images. Both types of AI-SHS exhibit a Cassie-Baxter wetting regime with comparable advancing and receding contact angles resulting in the landed drops rolling off instantly. The roughness parameter is preferably measured with atomic force microscopy yielding values of $r_{\text{E-AI/FS}}$ = 1.65 \pm 0.19 and $r_{\text{EA-AI/FS}}$ = 3.44 ± 0.07 , see Fig. 11d. The plastron shape and coverage are suitably estimated using digital still imaging and bright-field optical reflection microscopy on the submerged samples. Both E-AI/FS and EA-AI/FS exhibit highly reflective surfaces underwater due to plastrons that cover the entire specimen area. In contrast, the bright-field optical reflection microscopy images reveal a completely different plastron shape and solid-liquid area fraction. While the plastron on EA-Al/FS is continuous with randomly distributed round pinning points and a solid-liquid area fraction of $\varphi_s = 0.16 \pm 0.08$, see Fig. 11c1, the E-Al/FS demonstrated an irregular shape with a solid-liquid area fraction of only φ_s = 0.75 \pm 0.03, see Fig. 11c2. The latter is due to the deficiency of oxide/hydroxide groups resulting in the low FS coverage, which fails to form a thermodynamically stable plastron, i.e., with the liquid-air interface at the top of the asperities, see Fig. 11b. Finally, the MSCA (θ^{Si}_{MS}) was obtained previously for Ti-SHS and compared to the advancing (θ^{Al}_{Adv} = 121.9° \pm 3.4°) and receding $(\theta^{Al}_{Rec}$ = 74.9° \pm 5.7°) contact angles on the FS-coated polished Al samples. While the advancing contact angles on both surfaces are similar, the receding contact angle on the polished Al is much lower due to the higher surface roughness on AI. With the measured solid-liquid area fraction and roughness parameter, the critical contact angle was calculated according as $cos(\theta_c)$ = $(\phi_s$ - 1)/(r - ϕ_s) and was found to be θc = 93.5° for EA-AI/FS. By comparing the MSCA and critical contact angle, it is predicted that EA-AI/FS are in a stable Cassie-Baxter wetting regime, see Fig. 11e. Using $r > (-1)/(\cos(\theta)) + \varphi_s (1 + 1/(\cos(\theta))) = r_{min}$, the stability of plastron underwater is estimated on EA-AI/FS, also predicting stable plastron, see Fig. 11f.

30

35

50

[0039] As described, Figs. 11a1-h show an embodiment of applying the inventive method and predict corrosion resistance of Al samples. Fig. 11a1, a2 show scanning electron microscopy images of the E-Al/FS (Fig. 11a1) and EA-Al/FS (Fig. 11a2) samples. Fig. 11b shows energy-dispersive X-ray spectroscopy (EDS) measurements of the bare, E-Al/FS, and EA-Al/FS samples. Fig. 11c shows optical reflectance microscopy image of the E-Al/FS (Fig. 11d1) and EA-Al/FS (Fig. 11d2) samples immersed underwater to assess air plastron shape and surface coverage. Inset images are the static water contact angle measured on the E-Al/FS and EA-Al/FS surfaces. Fig. 11d shows 3D reconstruction AFM image of EA-Al/FS. Fig. 11e shows Lafuma and Quéré diagram demonstrating the stability of the Cassie-Baxter wetting regime built on the EA-Al/FS samples. Fig. 11f shows the Marmur diagram calculated for the bare and EA-Al/FS samples using the solid-liquid area fraction values as shown in Fig. 11c. Digital images showing (Fig. 11g) the bare Al and (Fig. 11h) EA-Al/FS samples which were recorded at days 0 and 234 of immersion in artificial seawater. The bottom images were captured at a grazing angle to prove the existence of plastron on the EA-Al/FS samples by their high reflectivity, in contrast to the bare Al samples that were severely corroded.

[0040] To evaluate the hypothesis of plastron stability, the corrosion resistance of the developed Al-SHS was examined. It is observed that Al is susceptible to corrosion in marine environments due to aggressive chloride ions. It is anticipated that the plastron, serving as a dielectric barrier, will improve the corrosion resistance of Al. Electrochemical measurements in an aqueous 3.5 wt.% NaCl electrolyte confirmed the remarkable corrosion protection of EA-Al/FS, while all other surfaces, spanning from super-hydrophilic to super-hydrophobic, showed only marginal improvements. Yet, such plastrons will be useful if SHS exhibits a long-lasting wetting-repellent performance. Therefore, the E-Al/FS, EA-Al/FS, and bare (B-Al, control) samples were immersed in artificial seawater. The bare Al samples corrode within the first 3 weeks (as shown in Fig. 11g), while the E-Al/FS exhibit pronounced corrosion products already after 16 days of immersion due to the loss of plastron and exposing high surface area substrates to a corrosive medium (as shown in Fig. 12a). After

120 days of immersion, the samples are massively corroded (Fig. 12b). At the same time, the EA-AI/FS exhibit corrosion-free performance even after ~8 months (234 days) of continuous immersion in seawater still demonstrating a highly reflective plastron (Fig. 11h). The EA-AI/FS substrates demonstrate 5 times longer infinite passive air trapping in highly corrosive seawater. This long-term immersion test provides evidence to support the hypothesis of corrosion protection for SHS due to (i) the stable and continuous plastron that eliminates contact of the highly corrosive media with the AI surface (Fig. 11h, bottom image), and (ii) the FS coating delays the onset of corrosion at the pinning points. At the same time, the wetting-repellent resistance of SHS with a metastable plastron is short-lived corroding rapidly due to their high surface area. This is distinct from goniometric measurements, which are unable to predict the corrosion performance of SHS based on the static apparent CA. Figs. 12a and b show the corrosion resistance of the E-AI/FS specimens immersed continuously in artificial seawater for (Fig. 12a) 16 and (Fig. 12b) 120 days.

[0041] In an exemplary embodiment, characterizing the surface 2 is achieved by the characterization of specific sets of features that are responsible for performance differences of SHS underwater for closely related treatment systems. Here, a facile reflectance microscopy technique is used as a first (rough) approximation. To demonstrate the general applicability of the method, two sets of SHS with plastron are prepared: (i) the same hydrophobic molecule coating but different anodized Ti surface morphologies, named Ti-SHS1-FS and Ti-SHS2-FS, see Figs. 13a-d, and Table 1 below, and (ii) the same anodized Ti surface morphology but different hydrophobic coatings, named Ti-SHS1-FS and Ti-SHS1-Sil (Table 2 below). The stability of the plastron and surface coverage were then assessed over time by immersing SHS in water as shown in Figs. 14a-m. The optical reflectance microscopy measurement provides plastron shape and surface coverage change over a millimeter scale range.

[0042] Figs. 13a, b show scanning electron (SEM) and Figs. 13c, d show atomic force microscopy images of Ti-SHS prepared by electrochemical anodization in (Figs. 13a, c) NaOH/ H_2O_2 (Ti-SHS1), and (Figs. 13b, d) in KOH/ K_3PO_4 (Ti-SHS2) aqueous electrolytes.

Table 1: an embodiment of an anodization protocol for the Ti-SHS1-FS and Ti-SHS2-FS surfaces.

| Protocol | Ti-SHS1 | Ti-SHS2 | |
|-----------------------------|--|-----------------------|--|
| Base Material 4 | Ti-6AI-4V | Ti-6Al-4V | |
| Aqueous Solution | 1.5 M NaOH/H ₂ O ₂ 0.11 M KOH + 0.02 M K ₃ P0 | | |
| Anodization Voltage V | 15 V for 30 min 30 V for 30 min | | |
| Counter electrode 8 | Stainless steel (316) | Stainless steel (316) | |
| Minimal roughness parameter | 2.48 ± 0.44 | 1.79 ± 0.05 | |

Table 2: two molecules used to create SHS on the anodized Ti alloy substrates.

| FS-100 (FS) | | Laureth-4 Phosphate (Silaphos, Sil) | |
|------------------------|-------------------------|-------------------------------------|--|
| agent shown in Fig. 15 | | agent shown in Fig. 16 | |
| Surface tension | 15.5 mN m ⁻¹ | 23 mN m ⁻¹ | |

[0043] In the case of Ti-SHS1-Sil, the basic condition is not fulfilled, see Fig. 14a-c, j, k. The MSCA, which was measured on the 100-nm-thick SiO2 on the Si wafer and functionalized with the laureth-4 phosphate (Sil) molecule, reveals considerably lower values as compared to the fluorinated surfactant (FS), indicating insufficient hydrophobicity of the coating, see Fig. 14m. Despite having a similar roughness parameter to Ti-SHS1-FS, but substantially lower most stable contact angle (MSCA), the Ti-SHS1-Sil surfaces always reside in the metastable region even at the lowest solid-liquid area fraction values, Fig. 14j. The latter explains the fact that the plastron on the Ti-SHS1-Sil samples degrades continuously overtime, eventually reaching homogeneous (Wenzel) wetting after 2 hours of immersion, Fig. 14c. In the case of Ti-SHS2-FS, Fig. 13b, d, the air bubbles, which formed spontaneously on the surface during the immersion process, disappeared within minutes. The plastron undergoes gradual decay for ~60 min before reaching a state of near stability, Fig. 14d-f, j, l. After 2 h, the plastron exhibits an irregular broken pattern surrounded by wet regions, Fig. 14i, dark regions. Such plastron performance is attributed to the partial fulfillment of thermodynamic conditions at the nanomicro-rough protrusions but not at the flat surrounding areas (Fig. 14l, inset image, and Fig. 13b, d). At the same time, Ti-SHS1-FS exhibit stable plastron for longer than 2 hours with minimal changes indicating the fulfillment of thermodynamic stability conditions on the Ti-SHS1-FS surfaces (Fig. 14g-i, j, m). The suggested metric can assess plastron stability within a reasonable timeframe, and thus, can be used even before measurements of more complex parameters

such as roughness, the MSCA, and plastron thickness.

[0044] Figs. 14a-I show plastron stability and (Fig. 14j) corresponding solid-liquid area fraction change as measured using optical reflectance microscopy imaging for (Figs. 14a-c) Ti-SHS1-Sil, (Figs. 14d-e) Ti-SHS2-FS, (Figs. 14g-i) Ti-SHS1-FS. The samples were immersed in water and the images were captured immediately. (Figs. 14k-m) Marmur diagrams for the (Figs. 14k) Ti-SHS1-Sil, (Figs. 14l) Ti-SHS2-FS, and (Figs. 14m) Ti-SHS1-FS samples. The solid-liquid area fraction in (Figs. 14k) is shown for time zero. Inset in (Figs. 14l) is the 3D reconstruction AFM image of the Ti-SHS2-FS sample. The yellow area in (Figs. 14k-m) covers all configurations of plastron based on the advancing and receding CAs measured on a flat surface and the roughness parameter of the corresponding SHS system.

10 List of Reference Numerals

[0045]

- 2 surface
- working electrode (anode)
 - 6 electrolyte
 - 8 counter electrode (cathode)
 - 10 fluorinated agent
 - 12 furnace
- 20 14 component
 - 16 plastron

Claims

25

30

35

40

55

- 1. Method for preparation of a surface (2), comprising the steps of:
 - a. Providing a material, preferably a metal-containing material, said material comprises the said surface (2);
 - b. Connecting the material as a working electrode (4);
- c. Providing an electrolyte (6);
 - d. Addition of H₂O₂ to the electrolyte (6);
 - e. Providing a counter electrode (8);
 - f. Applying a pre-defined voltage (V), wherein, upon application of the voltage (V), anodization of the working electrode (4) is carried out over a pre-defined time interval;
 - g. Functionalizing the material by bringing it into contact with a fluorinated agent (10) and heating it to a predefined temperature.
- 2. Method according to claim 1, wherein the material is a titanium alloy, preferably alpha-beta titanium aluminum vanadium alloy.
- **3.** Method according to claim 1, wherein the material is aluminum or an aluminum alloy.
- **4.** Method according to any one of claims 1 to 3, wherein the counter electrode (8) is made of steel.
 - **5.** Method according to any one of claims 1 to 4, wherein the electrolyte (6) is a NaOH solution.
- 6. Method according to any one of claims 1 to 5, wherein the pre-defined time-interval is at least 5 min, preferably at least 30 min.
 - Method according to any one of claims 1 to 6, wherein the pre-defined voltage (V) is 15 V +/- 5 V.
 - **8.** Method according to any one of claims 1 to 7, wherein the fluorinated agent (10) comprises or is a fluorinated phosphonic acid ester, preferably perfluoroalkyl phosphate acid ester.

- **9.** Method according to any one of claims 1 to 8, wherein the pre-defined temperature is in the range from 20 °C to 70 °C.
- **10.** Method for characterizing a surface (2), in particular a surface (2) which has been prepared using the method according to any one of claims 1 to 9, wherein the surface's (2) roughness, liquid-solid area fraction, and/or most stable, advancing and receding contact angles are measured, wherein a long-term stability of air trapping on the surface (2) is characterized based on the roughness, liquid-solid area fraction, and/or the most stable, advancing and receding contact angles.
- 10 **11.** Method according to any one of claims 1 to 10,

15

20

25

30

35

40

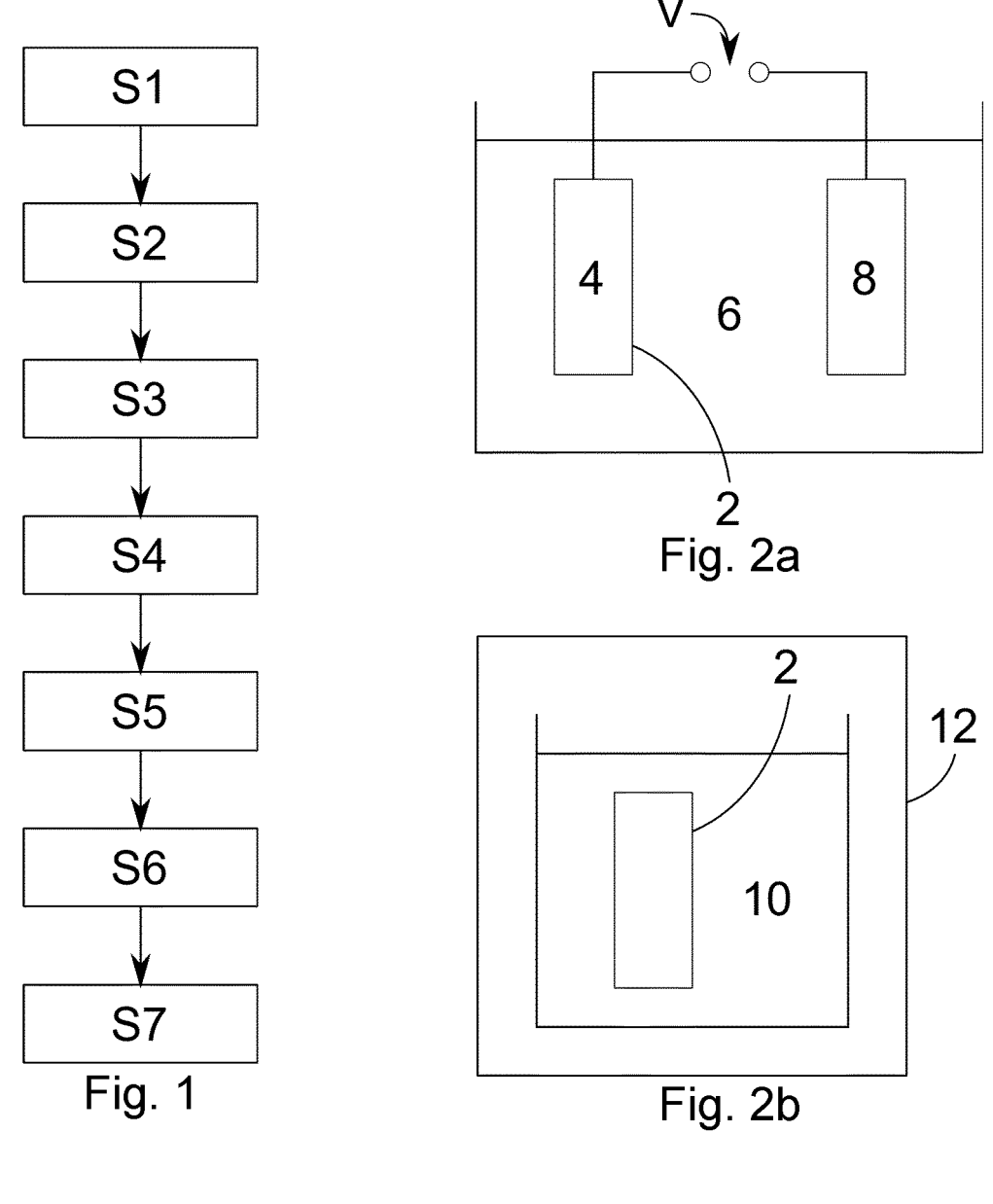
45

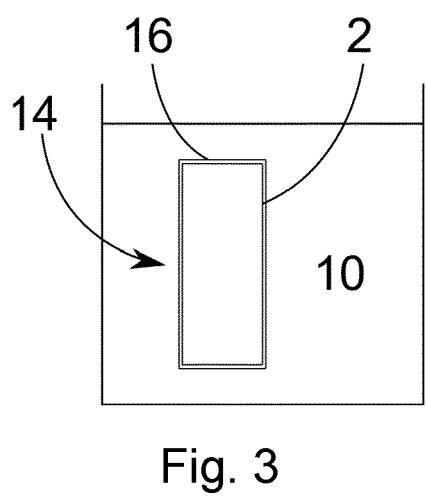
50

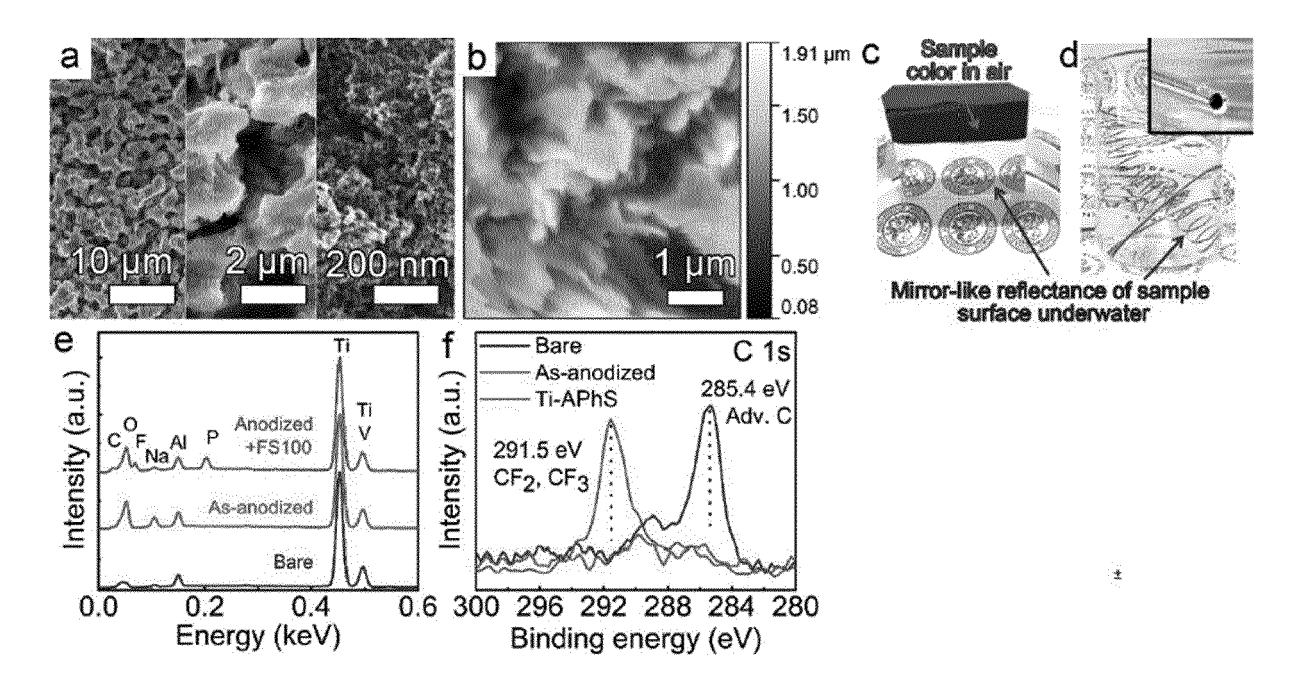
55

wherein the surface (2) is submerged in a liquid, upon which a plastron (16) forms on the surface (2), wherein shape of the plastron (16) and/or coverage of the surface (2) with the plastron (16) are estimated using optical reflection microscopy on the submerged surface (2).

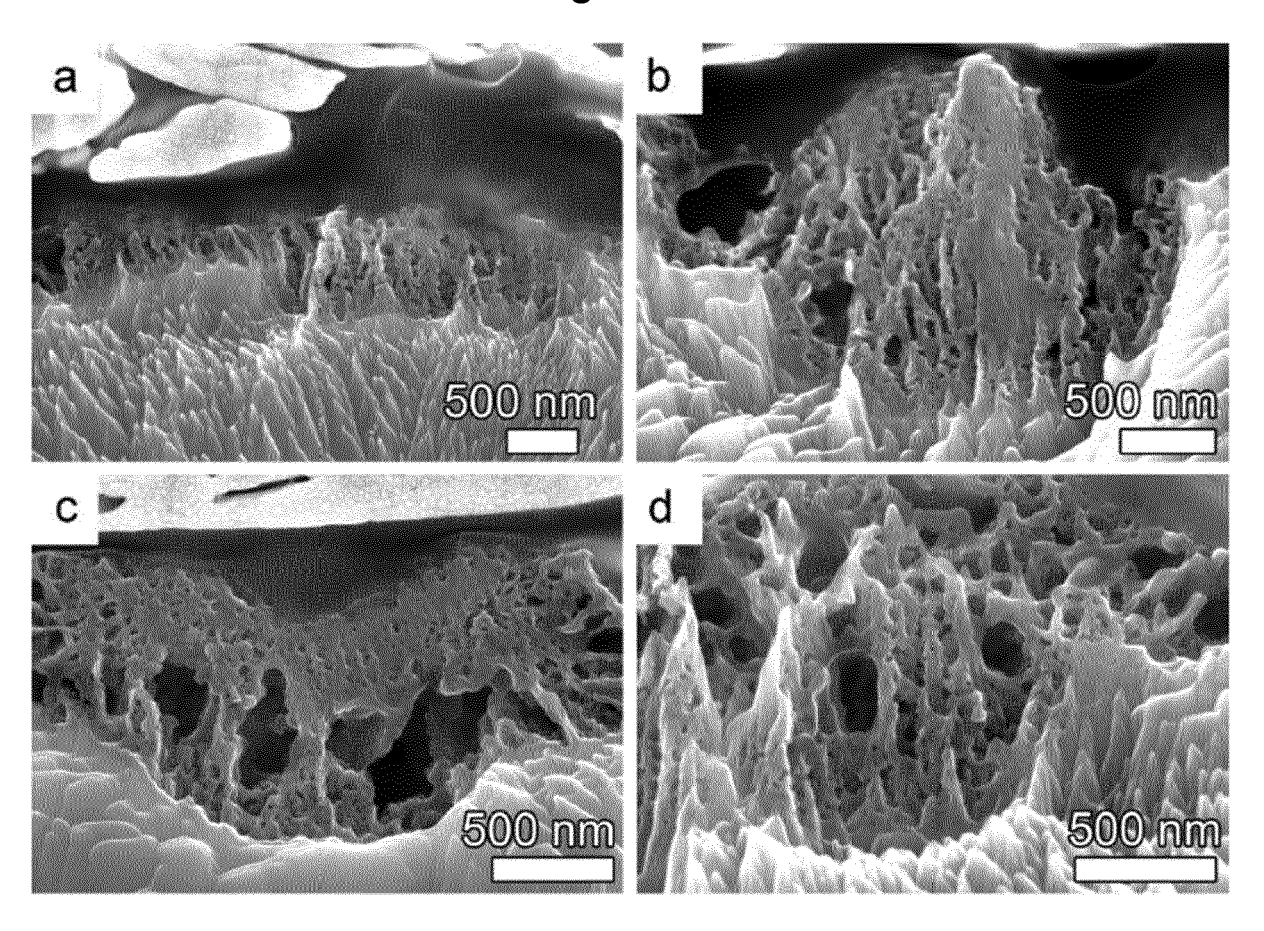
- **12.** Component (14), comprising a surface (2) which has been prepared using the method according to any one of claims 1 to 9.
- **13.** Component (14) according to claim 12, wherein the surface (2) is in a thermodynamically stable Cassie-Baxter state.
- **14.** Component (14), in particular according to claim 12 or 13, which comprises a surface (2) configured to be covered by a thermodynamically stable air layer when immersed in an aqueous medium.
- **15.** Use of a component (14) according to any one of claims 11 to 14 in a medical application, in an aerospace application, in a marine application, in an application in the chemical industry, or in an application in a gas turbine.







Figs. 4a-f



Figs. 5a-d

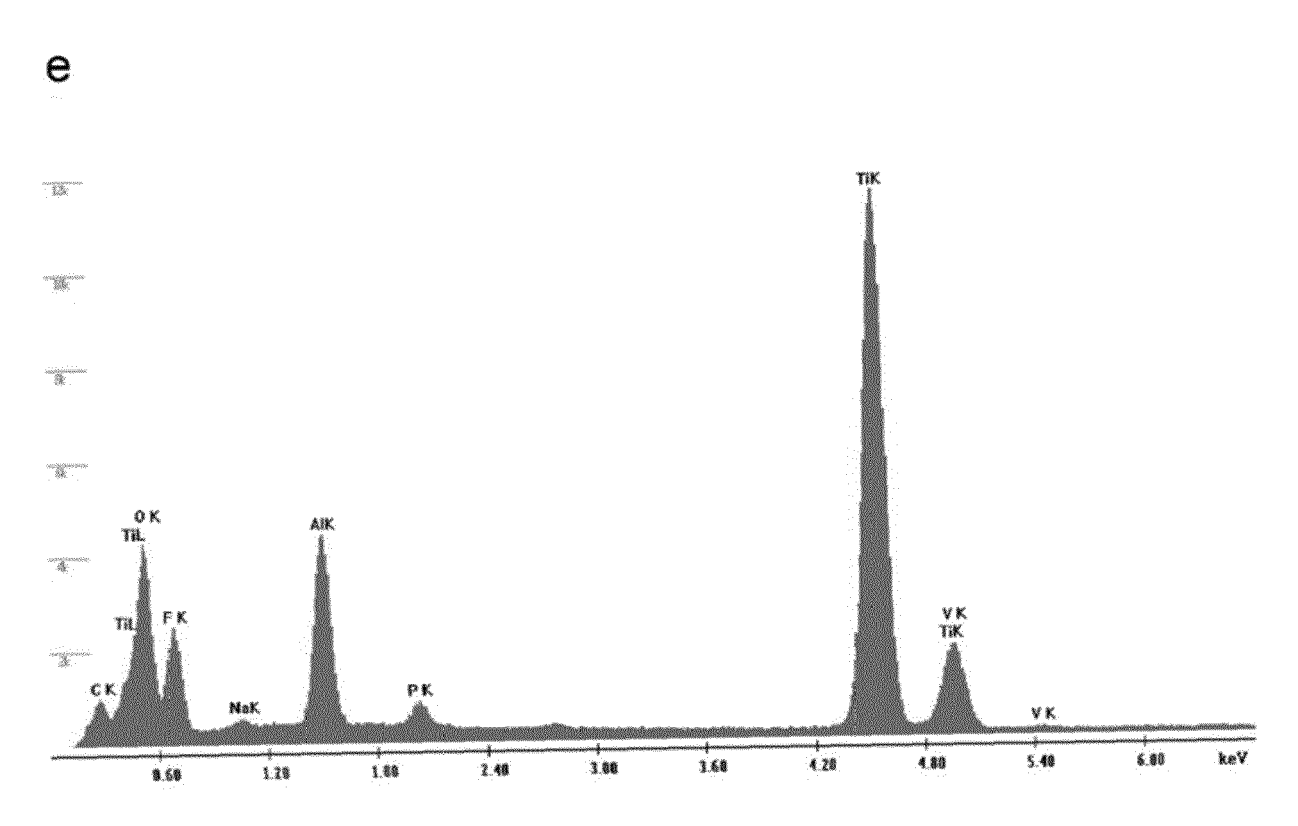
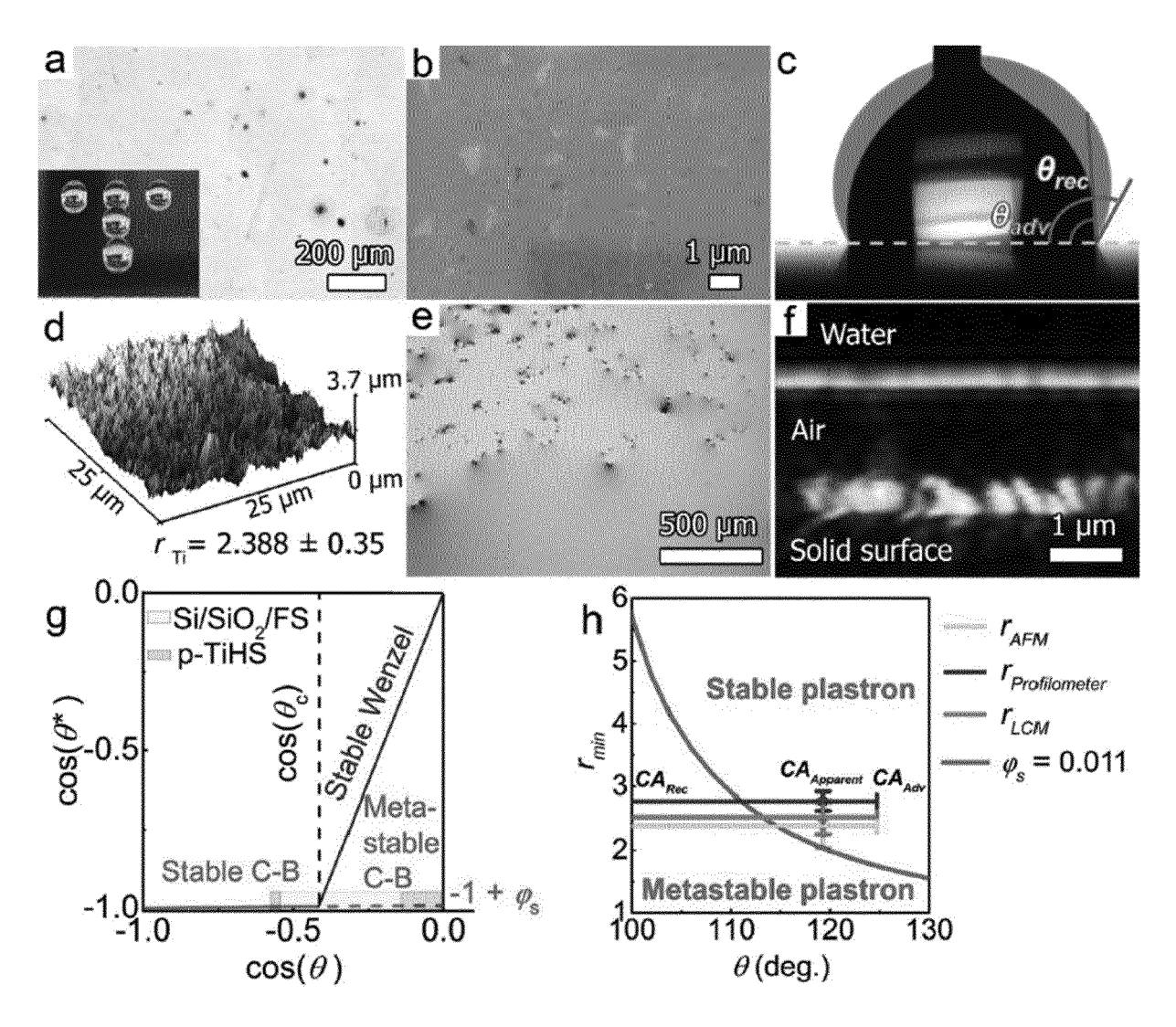
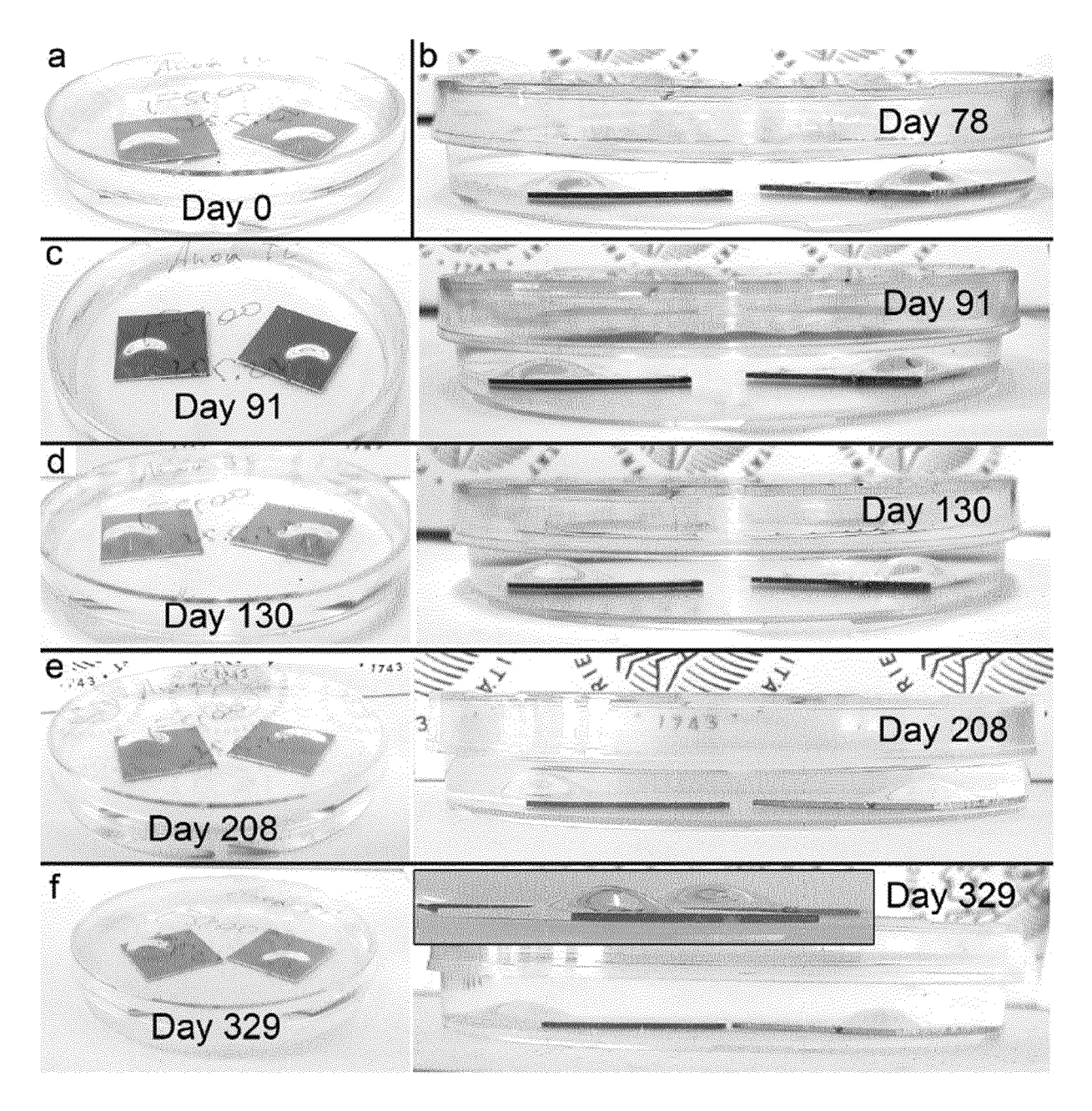


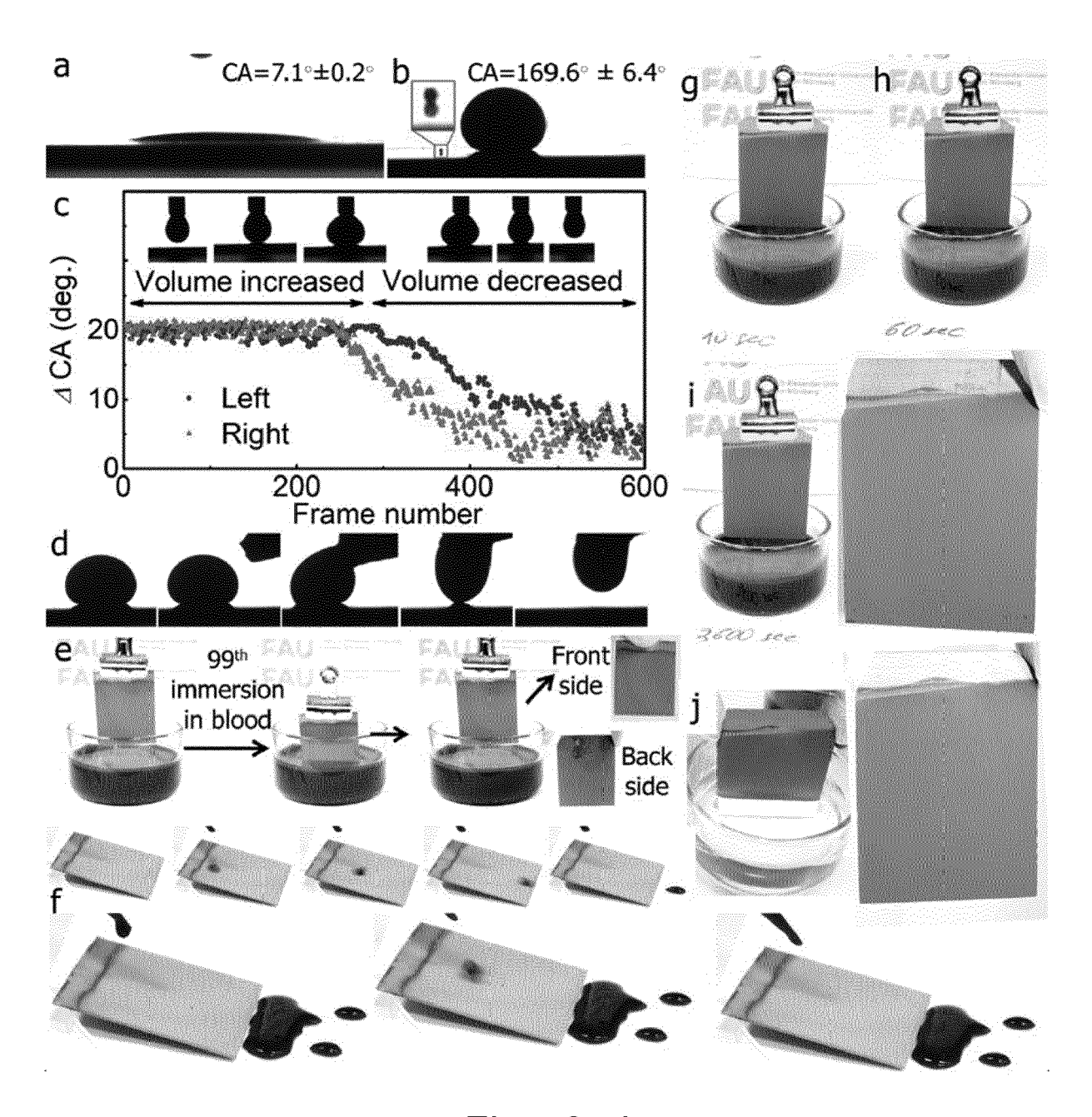
Fig. 5e



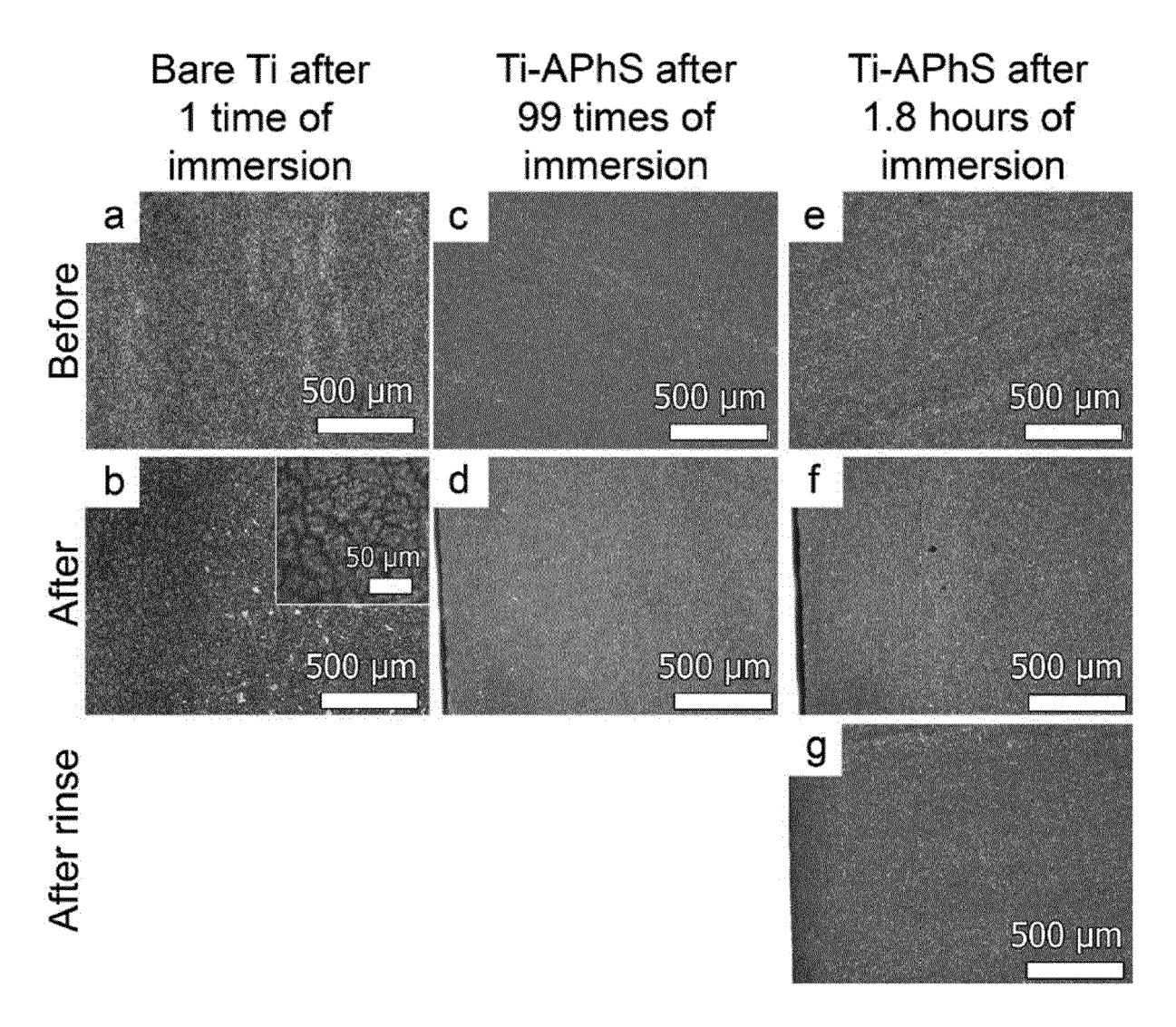
Figs. 6a-h



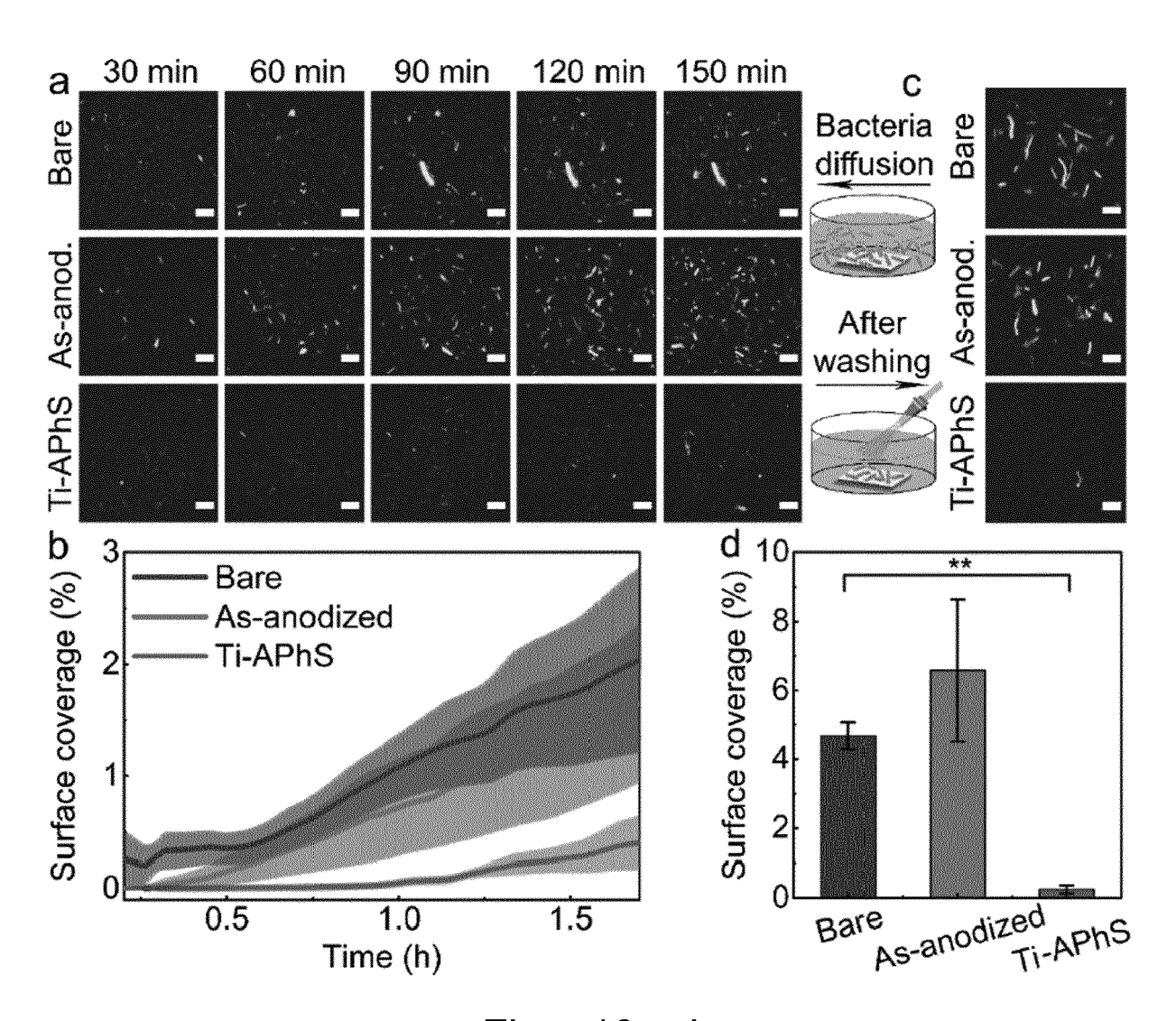
Figs. 7a-f



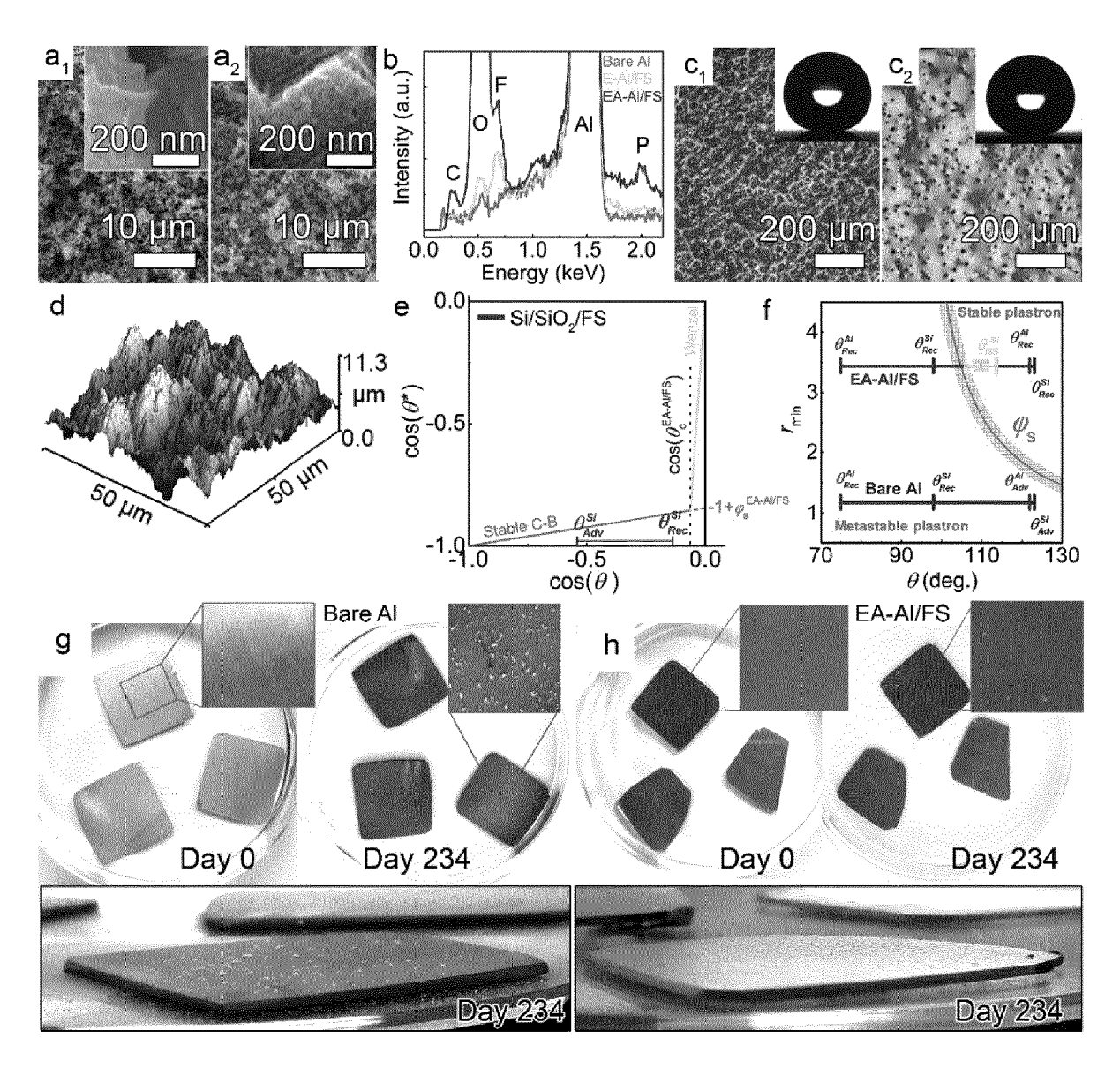
Figs. 8a-j



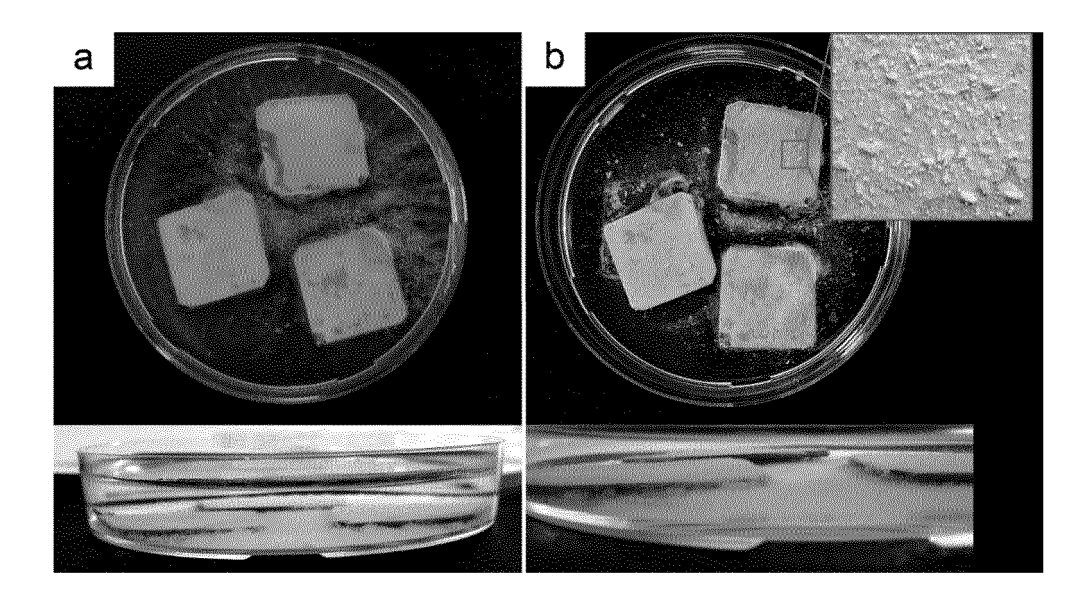
Figs. 9a-g



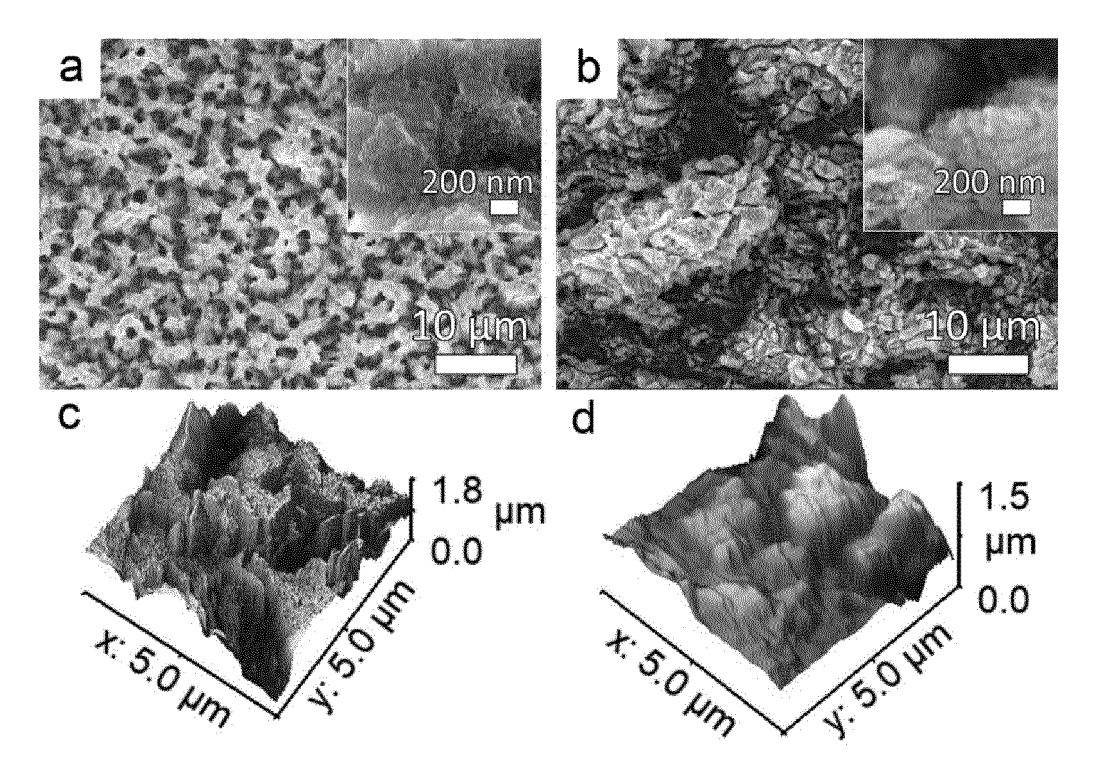
Figs. 10a-d



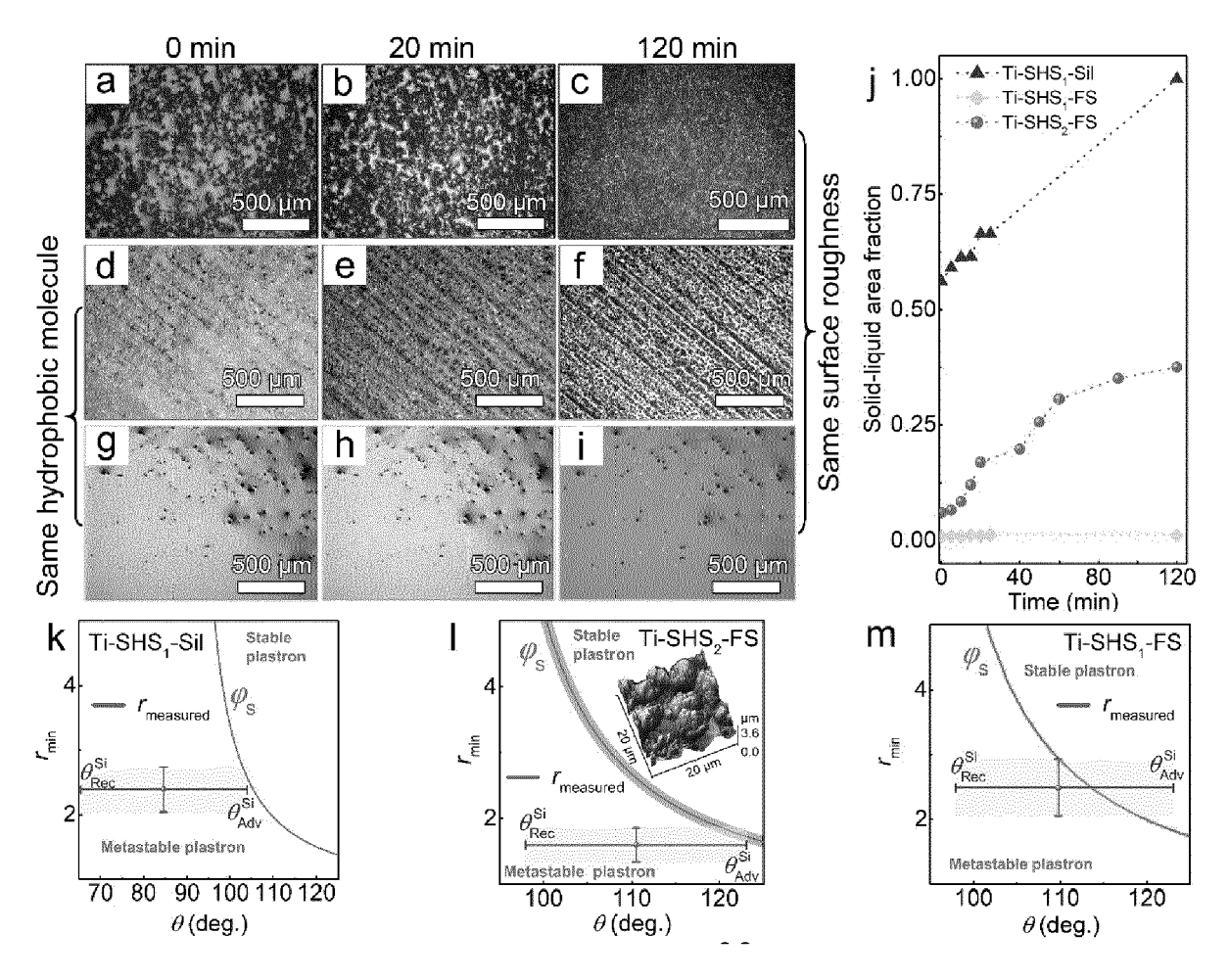
Figs. 11a1-h



Figs. 12a,b



Figs. 13a-d



Figs. 14a-m

F₃C
$$\begin{pmatrix} c \\ F_2 \end{pmatrix}_{5-9}$$
 O $\begin{pmatrix} c \\ F_2 \end{pmatrix}_{5-9}$ CF₃
Fig. 15

REFERENCES CITED IN THE DESCRIPTION

This list of references cited by the applicant is for the reader's convenience only. It does not form part of the European patent document. Even though great care has been taken in compiling the references, errors or omissions cannot be excluded and the EPO disclaims all liability in this regard.

Patent documents cited in the description

- US 20060029808 A1 [0005]
- US 20070005024 A1 [0005]

- US 201410238263 A1 [0005]
- CN 108486633 A [0005]

Non-patent literature cited in the description

- LU, Y. et al. Robust self-cleaning surfaces that function when exposed to either air or oil. Science, 2015, vol. 347, 1132-1135 [0003]
- LI et al. Challenges and strategies for commercialization and widespread practical applications of superhydrophobic surfaces. Science Advances, 2023, vol. 9 (42 [0003]
- GAO et al. Facile fabrication of superhydrophobic surfaces with low roughness on Ti-6Al-4V substrates via anodization. Applied Surface Science, 2014, vol. 314, 754-759 [0005]
- THAMARAISELVAN et al. Superhydrophobic candle soot as a low fouling stable coating on water treatment membrane feed spacers. ACS Appl. Bio Mater., 2021, vol. 4, 4191-4200 [0016]

- XU et al. Infinite lifetime of underwater superhydrophobic states. Phys. Rev. Lett., 2014, vol. 113, 136103 [0016]
- TESLER. Long-term stability of aerophilic metallic surfaces underwater. Nature Materials, 22 December 2023, 1548-1555 [0017]
- MARMUR, A. Underwater super-hydrophobicity: theoretical feasibility. Langmuir, 2006, vol. 22, 1400-1402 [0019]
- LAFUMA, A.; QUÉRÉ, D. Superhydrophobic states.
 Nat. Mater., 2003, vol. 2, 457-460 [0019]